Annals of Botany **125**: 459–469, 2020
doi: 10.1093/aob/mcz181, available online at www.academic.oup.com/aob

ANNALS OF BOTANY
Founded 1887

Ultrastructural and biochemical analyses reveal cell wall remodelling in lichen-forming microalgae submitted to cyclic desiccation–rehydration

María González-Hourcade[1], Marcia R. Braga[2], Eva M. del Campo[1], Carmen Ascaso[3], Cristina Patiño[4] and Leonardo M. Casano[1,*]

[1]University of Alcalá, Department of Life Sciences, 28871-Alcalá de Henares, Madrid, Spain, [2]Institute of Botany, Department of Plant Physiology and Biochemistry, 04301-012 São Paulo, SP, Brazil, [3]Museo Nacional de Ciencias Naturales, CSIC, Department of Biogeochemistry and Microbial Ecology, c/Serrano 115, 28006, Madrid, Spain and [4]Centro Nacional de Biotecnología, CSIC, c/Darwin 3, 28049, Madrid, Spain
For correspondence. E-mail leonardo.casano@uah.es2020125**3459470*

Received: 10 September 2019 Returned for revision: 15 October 2019 Editorial decision: 25 October 2019 Accepted: 29 October 2019
Published electronically 4 November 2019

• **Background and Aims** One of the most distinctive features of desiccation-tolerant plants is their high cell wall (CW) flexibility. Most lichen microalgae can tolerate drastic dehydration–rehydration (D/R) conditions; however, their mechanisms of D/R tolerance are scarcely understood. We tested the hypothesis that D/R-tolerant microalgae would have flexible CWs due to species-specific CW ultrastructure and biochemical composition, which could be remodelled by exposure to cyclic D/R.
• **Methods** Two lichen microalgae, *Trebouxia* sp. TR9 (TR9, adapted to rapid D/R cycles) and *Coccomyxa simplex* (Csol, adapted to seasonal dry periods) were exposed to no or four cycles of desiccation [25–30 % RH (TR9) or 55–60 % RH (Csol)] and 16 h of rehydration (100 % RH). Low-temperature SEM, environmental SEM and freeze-substitution TEM were employed to visualize structural alterations induced by D/R. In addition, CWs were extracted and sequentially fractionated with hot water and KOH, and the gel permeation profile of polysaccharides was analysed in each fraction. The glycosyl composition and linkage of the main polysaccharides of each CW fraction were analysed by GC–MS.
• **Key Results** All ultrastructural analyses consistently showed that desiccation caused progressive cell shrinkage and deformation in both microalgae, which could be rapidly reversed when water availability increased. Notably, the plasma membrane of TR9 and Csol remained in close contact with the deformed CW. Exposure to D/R strongly altered the size distribution of TR9 hot-water-soluble polysaccharides, composed mainly of a β-3-linked rhamnogalactofuranan and Csol KOH-soluble β-glucans.
• **Conclusions** Cyclic D/R induces biochemical remodelling of the CW that could increase CW flexibility, allowing regulated shrinkage and expansion of D/R-tolerant microalgae.

Key Words: Cell wall, cell wall folding, cell wall remodelling, *Coccomyxa*, desiccation, desiccation tolerance, lichen, microalgae, *Trebouxia*.

INTRODUCTION

Lichens are mutualistic symbiotic systems in which at least two different organisms coexist: a fungus (mycobiont) and one or more photosynthetic partner that can belong to the cyanobacteria (cyanobiont) and/or the green algae (phycobiont). In some of these systems, the presence of two or more microalgae (Casano *et al.*, 2011), bacteria (Molins *et al.*, 2013) or yeasts (Aschenbrenner *et al.*, 2014) has recently been described. Lichens are found in a variety of environments that range from mild habitats such as humid tropical forests (Aragón *et al.*, 2016) to extreme ecosystems such as the Arctic (Ascaso *et al.*, 1990; Zhang *et al.*, 2015) and hot deserts (Vargas Castillo *et al.*, 2017), where vascular plants cannot grow (Fritsch and Haines, 1923; Belnap *et al.*, 2001).

Lichens and their green microalgae have both been described as poikilohydric organisms, meaning that they do not actively regulate their water content; consequently, they depend on the availability of water in the environment. Lichens can be exposed to long periods of water shortage, which causes protoplast desiccation, a potentially strong abiotic stress (Kranner *et al.*, 2008). When water becomes available again, the lichen thallus rehydrates, and after the first few minutes or hours of rehydration active metabolism is restored (Schroeter *et al.*, 1992; Tuba *et al.*, 1996). Accordingly, these organisms, adapted or acclimatized to alternating desiccation–rehydration (D/R) cycles, have developed desiccation tolerance (DT), defined as a set of strategies to cope with these extreme conditions, which permit survival with a cellular water content of ~5–10 % (Gaff, 1971; Holzinger and Karsten, 2013), in some cases for long periods (Kranner *et al.*, 2008).

Ramalina farinacea is an epiphytic fruticose lichen that is widely distributed in Mediterranean environments and is adapted to continuous rapid cycles of diurnal and/or seasonal desiccation and rehydration (Casano *et al.*, 2011) with an average relative humidity (RH) of ~25–30 %. *Solorina saccata* is a foliose lichen with a geographical distribution that encompasses

mild and cold areas, where it is normally protected in cracks of calcareous rocks, which predominantly present microenvironments with an RH of 55–60 % (during the dry season) or more. In a previous study (Centeno *et al.*, 2016), we studied the physiological responses of two lichen microalgae with a contrasting habitat preference, when exposed to desiccation below 25–30 % RH and then rehydrated. These were *Trebouxia* sp. TR9 (TR9), isolated from *R. farinacea*, and *Coccomyxa simplex* (Csol), obtained from *S. saccata*. The relative water content and water potential were recorded throughout the process together with sugar and primary metabolite profiles. Under these experimental conditions, both desiccation and rehydration occurred more rapidly in Csol than in TR9. Metabolomic analyses showed notable differences between the two microalgae, whereby TR9 was constitutively richer in polyols and capable of increasing synthesis of osmo-compatible solutes during desiccation, whereas Csol increased polyol synthesis under D/R. Although both microalgae are desiccation-tolerant, in TR9 this capacity seems to rely mainly on constitutive features, whereas in Csol a higher proportion of inducible mechanisms appears to play a role in DT.

The most studied desiccation-tolerant organisms are those known as 'resurrection plants', a group of angiosperms that activate physiological, structural and biochemical responses to cope with desiccation stress (Farrant *et al.*, 2017 and references therein). These plants and some charophyte algae have evolved flexible cell walls (CWs), with distinctive biochemical and ultrastructural features, that fold as the protoplast shrinks due to dehydration and expand during rehydration (Moore *et al.*, 2008*a*,*b*; Holzinger and Pichrtová, 2016). The immediate consequence of this CW flexibility is to prevent the mechanical stress occurring during dehydration in cells with a relatively rigid CW, which damages the subtle connections between plasma membrane and wall (Sherwin and Farrant, 1996; Vicré *et al.*, 2004; Moore *et al.*, 2006). Recently, Farrant *et al.* (2017) reported that the flexibility of the CWs of the resurrection plant *Craterostigma wilmsii* seems to increase under desiccation conditions due to changes in glycosyl composition and the molecular size of xyloglycans. The 'controlled collapse' of CWs and changes in CW thickness have also been observed in the green microalga *Klebsormidium* (Streptophyta) under similar conditions (Holzinger and Karsten, 2013).

Few studies have been conducted on CW polysaccharide composition in lichen-forming algae. Besides a very low content (or even absence) of cellulose, the predominance of β-galactofuranans has been reported in the photobionts of *Ramalina gracilis* and *Cladina confusa* (Cordeiro *et al.*, 2005, 2007). More recently, we analysed the ultrastructure and polysaccharide composition of the microalgae of *R. farinacea*. Two green microalgae (*Trebouxia jamesii* and TR9) with different CWs (Casano *et al.*, 2011) coexist in this epiphytic lichen. At the ultrastructural level, we observed four clearly differentiable layers in the *T. jamesii* CW, whereas TR9 showed a more diffuse structure in which only three layers could be distinguished. Fractionation of *T. jamesii* and TR9 CWs revealed a high proportion of galactose, xylose and rhamnose that was associated with a β-xylorhamnogalactofuranan present in the hot water fraction. Meanwhile, the alkaline fraction showed high proportions of galactose, glucose and mannose similar to those found in *Asterochloris erici* (Cordeiro *et al.*, 2007). In addition, a comparative analysis of TR9 and Csol CWs indicated that although both CWs had the same number of layers (three), these were thinner and more defined in Csol than in TR9 (Casano *et al.*, 2011, Álvarez *et al.*, 2015). Furthermore, glucose, mannose, galactose and rhamnose were the predominant monosaccharides in Csol, in contrast to the glycosyl composition of the TR9 CW. Some genera of Trebouxiophyceae, such as *Coccomyxa*, also present algaenans, highly aliphatic, insoluble, non-enzymatically hydrolysable biopolymers previously known as sporopollenin (Zhang and Volkman, 2017), in the outermost layer of their CWs (Honegger, 2012 and references therein). Algaenans could play a role associated with resistance to biotic and desiccation stress (Dunker and Wilhelm, 2018). The distribution of algaenans in the class Trebouxiophyceae is not uniform, since they have been found in the CWs of some species of *Coccomyxa* and *Myrmecia*, but their presence is controversial in the *Trebouxia* genus (Honegger and Brunner, 1981; König and Peveling, 1984).

It should be noted that analyses of algal CWs in general, and those of lichen microalgal CWs in particular, have primarily been performed with cells under control (hydrated) conditions rather than the cyclic D/R conditions that often occur in natural lichen habitats. This practice may fail to detect information on the degree of DT or acclimation responses. Therefore, our hypothesis was that lichen microalgae such as TR9 and Csol with distinctive DT strategies, probably resulting from adaptation/acclimation to contrasting environments, would have flexible CWs. However, this mechanical feature might vary between these two microalgae due to species-specific ultrastructural arrangement and biochemical composition, which in turn might be remodelled by exposure to cyclic D/R. In consequence, the aim of the present study was to investigate whether these lichen microalgae are capable of folding and expanding their CWs following protoplast contraction and expansion due to exposure to desiccation and rehydration, respectively. In addition, we sought to determine possible acclimation changes in CW polysaccharides after exposure to cyclic D/R in which each alga was desiccated under conditions similar to those found in their natural habitats (25–30 % RH for TR9, 55–60 % for Csol).

MATERIALS AND METHODS

Microalga isolation and culture

Trebouxia sp. TR9 microalga was isolated from the lichen *Ramalina farinacea* collected at Sª El Toro (Castellón, Spain; 39°54′16″ N, 0°48′220″ W) (Gasulla *et al.*, 2010). *Coccomyxa simplex* (formerly *C. solorinae-saccatae*, strain 216-12) was obtained from the SAG Culture Collection of Algae (Sammlung von Algenkulturen) at Göttingen University (Germany). According to this algal bank, Csol was isolated from the lichen *Solorina saccata* found in Großer St Bernhard, Switzerland (45°57′4″ N, 7°12′32″ W). Both microalgae were cultured under axenic conditions on small nylon squares (4 cm^2) in semisolid supplemented Bold 3N medium (Bold and Parker, 1962), inside a growth chamber at 15 °C under a 14-h/10-h light/dark cycle (light conditions: 25 µmol m^{-2} s^{-1}).

D/R treatment

Nylon squares containing 3-week-old cultures of Csol and TR9 (~180–200 and 200–300 mg FW, respectively) were removed from the culture medium and placed in a climatic chamber (K110; Pol-eko-Aparatura, Poland) for the four D/R cycles. The desiccation conditions, established as optimal for each microalga in previous experiments (Hell *et al.*, 2019), were 25–30 % RH for TR9 and 55 % RH for Csol cultures at 25 °C for 8 h. Afterwards, the cultures were transferred to Petri dishes with a semisolid medium, composed of 1.5 % agar in distilled water, at 100 % RH and 20 °C for 16 h. At the indicated times, samples were collected from the desiccation or rehydration treatment and weighed prior to subsequent microscopic analyses or CW extraction. Fully hydrated cells prior to D/R cycles were considered the control condition.

Structural analyses

For transmission electron microscopy (TEM) analysis, TR9 and Csol samples before and after four D/R cycles (in desiccated and rehydrated state) were high-pressure-frozen and freeze-substituted (Aichinger and Lütz-Meindl, 2005) with modifications. Samples were frozen in a Leica EM PACT2 high-pressure freezer and freeze-substituted with 1.5 % osmium tetroxide in acetone for 54 h at −90 °C then 4 h at −30 °C and 2 h at 4 °C in a Leica AFS2 freeze-substitution apparatus. After three washes with anhydrous acetone, samples were embedded in Epon 812 resin at room temperature and polymerized for 48 h at 60 °C. Seventy-nanometre sections were obtained in a Leica EM UC6 ultramicrotome and mounted on 200 mesh nickel grids, post-stained with 2 % (w/v) aqueous uranyl acetate and 2 % lead citrate and observed with a JEOL JEM 1011 (100 kV) electron microscope equipped with a Gatan Erlangshen ES1000W digital camera.

For low-temperature scanning electron microscopy (LTSEM), microalgae were observed by high-resolution field emission gun scanning electron microscopy (FEG-SEM) at low temperature before and after one cycle of D/R (in desiccated and rehydrated state). An AQUILO cryo preparation chamber (PP3010T, Quorum Technology) was connected to the FEG-SEM. Small samples of algal cultures were mounted using a mixture of 50 % Tissue Tek/50 % colloidal graphite and rapidly frozen under vacuum conditions. The cryo preparation chamber was maintained under high vacuum and cooled during fracturing, sublimation of surface ice and metal and carbon coating. Then, samples were transferred to a cold stage in the SEM chamber for FEG-ESEM analysis under cryogenic conditions.

Environmental scanning electron microscopy (ESEM) can be used to record secondary images under conditions of water vapour pressure and temperature up to water saturation (RH = 100 %). Algal samples were mounted on the stainless-steel stub with double-sided carbon adhesive and left to equilibrate at 5 °C for 15 min and then subjected to eight controlled vapour-pressure purges (from 99–100 % to 10 % and then from 10 % to 100 % RH), allowing the samples to equilibrate for several minutes at each RH level. Images were taken at each RH level. Samples of Csol were observed using a FEI Quanta 400 instrument under conditions of 15 kV acceleration potential and at a working distance of 5–10 nm. Samples of TR9 were visualized by means of field-emission gun high resolution ESEM (FEG-ESEM), using a QuemScan650F model (FEI, Netherlands) in environmental mode (10–4000 Pa). For this purpose, the GESED detector and 5–10 kV acceleration potential was applied.

The presence/absence of algaenans in the CW of both algal species was assessed by light microscopy (Eclipse Ci-L; Nikon) after crystal violet staining according to Zych *et al.* (2009).

Extraction and fractionation of CW components

After extraction of the extracellular polymeric substances attached to the external surface of the CW (Casano *et al.*, 2015), Csol and TR9 microalgae (1–5 g FW) were subjected to four cycles in a French press (1350 psi), which disrupted 95 % of the control cells in both algae. However, in cells exposed to D/R conditions, disruption was slightly less efficient since we observed a higher proportion of unbroken cells (~10–15 %). Cell walls were pelleted (10 000 *g*, 15 min at 4 °C) and washed with 30 mL of 100 mM NaCl and twice with ultrapure water. Cell debris was removed by successive washes with organic solvents: three times with 93 % ethanol (20 mL g^{-1} FW), once at room temperature overnight, once under the same conditions for 2 h and once at 80 °C with gentle stirring for 2 h; twice with chloroform:methanol 1:1 (v/v) (20 mL g^{-1} FW) with stirring for 1 h; and twice with pure acetone at room temperature for 8 h each time. Cell walls were filtered through glass-fibre filters (Merck Millipore), dried in an oven at 60 °C for 2 d and weighed.

Cell walls of TR9 and Csol were fractionated by successive extraction with ultrapure hot water (HW) and 10 % KOH (KOH) (Cordeiro *et al.*, 2005). Briefly, 120 mg of CW was suspended in 9 mL of ultrapure water and stirred at 100 °C for 4 h and then centrifuged (14 500 *g*, 5 min). This procedure was performed twice and the supernatants were combined, dialysed, freeze-dried and considered as the HW-soluble fraction. The insoluble material was suspended in 9 mL of 10 % KOH and maintained at room temperature overnight with gentle agitation. After centrifugation (14 500 *g*, 5 min), the insoluble material was re-extracted by stirring with 10 % KOH at 100 °C for 4 h. Combined KOH supernatants were neutralized with acetic acid and precipitated with 3 volumes of 93 % ethanol at 4 °C overnight. After centrifugation (21 000 *g*, 5 min) and washing with 93 % ethanol, the precipitate was dried, re-solubilized in ultrapure water and considered as the KOH-soluble fraction. Total neutral sugars were determined by the phenol-H_2SO_4 method (Dubois *et al.*, 1956) using glucose as standard.

Gel-permeation chromatography

Aliquots of HW- and KOH-soluble fractions (~2 mg of neutral sugars) were added to a 70.0 × 1.6 cm (ID) Sepharose 4B column C (General Electric Healthcare) equilibrated with 150 mM phosphate–citrate buffer (pH 5.2) and eluted with the same buffer. The amount of neutral carbohydrates in each 2-mL fraction was determined as described above. Dextrans of 9.3, 76, 156 and 2000 kDa (Sigma–Aldrich, St Louis, MO, USA)

were used as standards for column calibration. Based on the carbohydrate amounts recovered from the column, the most prominent peaks were selected. In cases of CW fractions with polydisperse profiles, we selected the fractions with the highest mass. Therefore, ten eluted peaks from HW- and KOH-soluble fractions from control and D/R TR9 and Csol algae were dialysed (cut-off 2000 kDa) against bi-distilled water and lyophilized to perform glycosyl composition and glycosyl linkage analyses.

Glycosyl composition analysis

Glycosyl composition of selected fractions was analysed by combined gas chromatography–mass spectrometry (GC–MS) of the per-*O*-trimethylsilyl derivatives of the monosaccharide methyl glycosides produced from the samples by acidic methanolysis as described previously by Santander *et al.* (2013). Briefly, ~100–400 µg of the sample was heated with 1 M HCl in MetOH at 80 °C for 17 h. Then, a re-N-acetylation was carried out with a mixture of MetOH, pyridine and acetic anhydride for 30 min. The solvents were evaporated and the samples were derivatized with Tri-Sil® (Pierce) at 80 °C for 30 min. The GC–MS analysis of the per-*O*-trimethylsilyl methyl glycosides was performed using an Agilent 7890A GC interfaced to a 5975C MSD, equipped with a Supelco Equity-1 fused silica capillary column (30 m × 0.25 mm ID).

Glycosyl linkage analysis

Six of the ten samples contained sufficient sample mass (~1 mg) to perform a glycosyl linkage analysis. These samples were permethylated and reduced twice and acetylated, and the resulting partially methylated alditol acetates were analysed by GC–MS according to Heiss *et al.* (2009) with a slight modification. Briefly, the samples were suspended in dimethyl sulphoxide and stirred for 1 d and then permethylated using potassium dimsyl anion and iodomethane, and, in the case of uronic acids, reduced with lithium borodeuteride. After sample clean-up, permethylated material was subjected to two rounds of treatment with sodium hydroxide (15 min) and methyl iodide (45 min). The permethylated material was hydrolysed using 2 M trifluoroacetic acid (2 h at 121 °C), reduced with sodium borodeuteride and acetylated using acetic anhydride/trifluoroacetic acid. The resulting partially methylated alditol acetates were analysed using an Agilent 7890A GC interfaced to a 5975C Mass Selective Detector in electron impact ionization mode; separation was performed in a 30-m Supelco SP-2331 bonded-phase fused silica capillary column.

RESULTS AND DISCUSSION

Structural changes during D/R in lichen microalgae

Compelling evidence has been reported in recent years of a positive causal relationship between the response of plants and algae to water deficit and the biophysical properties of their CWs (Moore *et al.*, 2008*a*,*b*; Shtein *et al.*, 2018). The first step of our investigation was to analyse the ultrastructural modifications occurring during desiccation and rehydration of fully hydrated TR9 and Csol cells.

Desiccation/rehydration-induced structural alterations in TR9 and Csol, especially in their CW and plasma membrane, were visualized by TEM, LTSEM and ESEM (Figs 1–5). The TEM and LTSEM images of TR9, taken after four and one D/R cycle(s) respectively, showed that desiccation caused progressive cell shrinkage and CW deformation, which could be rapidly reversed when water availability increased (Fig. 1A–F and Supplementary Data Fig. S1). These changes were also observed in Csol (Fig. 2A–F), even though this latter microalga seemed to recover to a slightly lesser extent upon rehydration compared with TR9 since several cells did not completely expand. This difference in degree of recovery after desiccation linked to CW features was also found when employing ESEM, which permits rapid changes in the RH to which cells are exposed during microscope observation (Fig. 3). Under these conditions, TR9 tolerated an RH as low as 10 % and recovered after desiccation for up to five relatively rapid D/R cycles (entire cycle 20–25 min) (Fig. 3, upper panels). In contrast, Csol did not tolerate such drastic desiccation conditions, requiring a higher RH (60–65 %) during desiccation in order to recover upon rehydration (Fig. 3, lower panels). These findings suggest that TR9 is better adapted to rapid changes in water status, whereas Csol seems to need slower desiccation, probably in order to activate certain tolerance features. Irrespective of this, when desiccation was conducted at RH or speed similar to that encountered in their respective habitats, TR9 (Fig. 4 and Supplementary Data Fig. S2) and Csol (Fig. 5) plasma membranes remained in close contact with the deformed CW.

Crystal violet staining revealed a profound difference in CW permeability between TR9 and Csol, as only 21 % of Csol cells allowed dye entry whereas almost all TR9 cells became stained (Supplementary Data Fig. S3). Since algaenan hinders the penetration of large molecules of crystal violet (Zych *et al.*, 2009), our result indicates the absence of this biopolymer in the TR9 CW and its presence in Csol. These findings support those reported by Honegger (2012) regarding the presence of algaenan in *Coccomyxa* microalgae. However, the presence of algaenan in the algal CW of *Trebouxia* species remains controversial. König and Peveling (1984) have reported its presence in several *Trebouxia* species, but Honegger and Brunner (1981) did not find any acetolysis-resistant material, a characteristic of algaenan, in almost the same algal species. Our results clearly indicate that the CW of *Trebouxia* sp. TR9 species did not contain this highly resistant polymer and they therefore support the notion that the presence of algaenans is associated with typical trilaminar CWs, such as those of *Coccomyxa* species. In addition, we observed that the presence/absence of algaenan in Csol and TR9 was not modified by exposure to cyclic D/R (data not shown).

The diffuse trilaminar organization of the TR9 CW observed before D/R was preserved during desiccation (Fig. 4 A, B, D, E). However, after rehydration the inner and outermost layers (L1 and L3, respectively) became thinner while the intermediate layer (L2) became slightly thicker, so that the entire CW appeared to have a relatively more defined trilaminar structure, although total CW thickness did not change

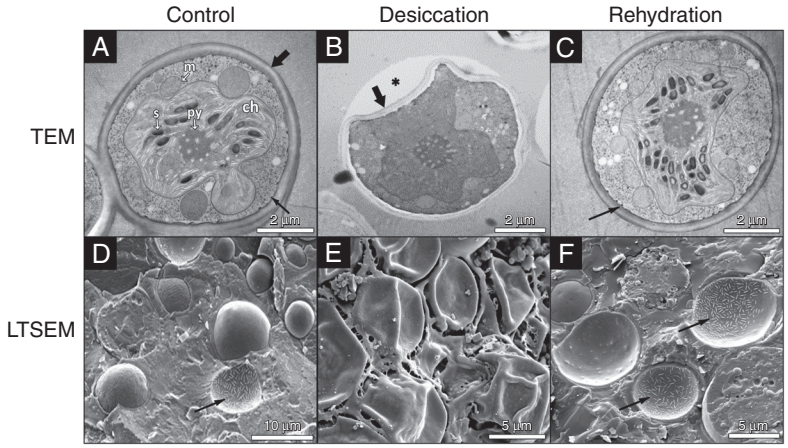

FIG. 1. TEM and LTSEM micrographs of *Trebouxia sp.* TR9 exposed to cyclic D/R. For TEM, TR9 cells were exposed to no D/R cycles (control, A) or four D/R cycles (desiccation, B; rehydration, C). For LTSEM, TR9 cells were exposed to no D/R cycles (control, D) or a single D/R cycle (desiccation, E; rehydration, F). Thick arrows indicate the CW and thin arrows mark plasmalemma invaginations. The asterisk in (B) indicates a gap between the Epon 812 resin and the CW, probably due to reduced adherence of the collapsed regions to the resin. Abbreviations in (A): ch, chloroplast; m, mitochondrion; py, pyrenoid; s, starch.

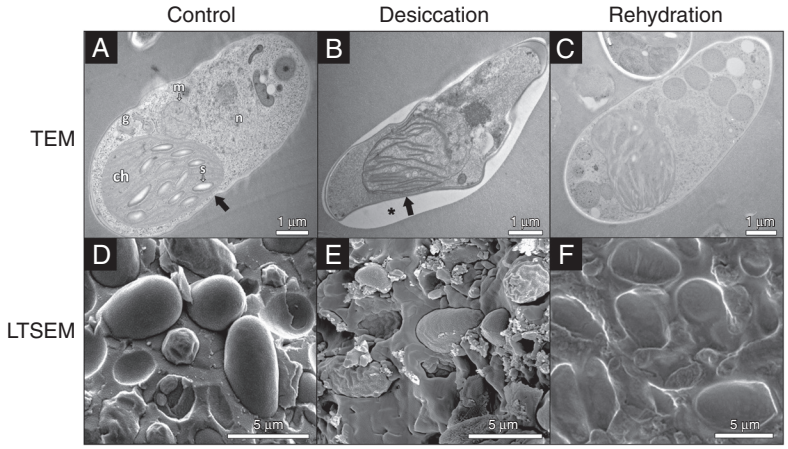

FIG. 2. TEM and LTSEM micrographs of *Coccomyxa simplex* exposed to cyclic D/R. For TEM, Csol cells were exposed to no D/R cycles (control, A) or four D/R cycles (desiccation, B; rehydration, C). For LTSEM, Csol cells were exposed no D/R cycles (control, D) or a single D/R cycle (desiccation, E; rehydration, F). Thick arrows indicate the CW. The asterisk in (B) indicates a gap between the Epon 812 resin and the CW, probably due to reduced adherence of the collapsed regions to the resin. Abbreviations in (A): ch, chloroplast; g, Golgi apparatus; m, mitochondrion; n, nucleus; s, starch.

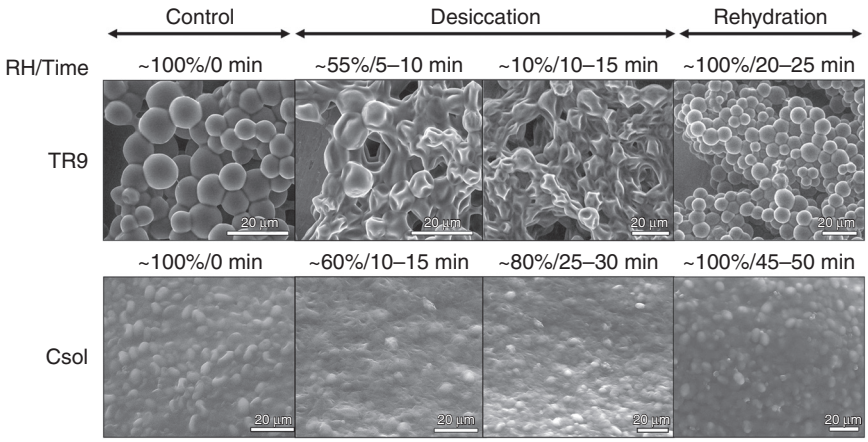

FIG. 3. ESEM micrographs of TR9 and Csol during a D/R cycle. Algal samples were left to equilibrate at 5 °C for 15 min and then subjected to eight controlled vapour pressure purges (from 99–100 % up to 10 % and then from 10 % to 100 % RH), allowing the samples to equilibrate for several minutes at each RH level. Images in the figure depict the key stages, timing and RH conditions during a D/R cycle, including the lowest RH below which Csol did not normally rehydrate, under ESEM conditions.

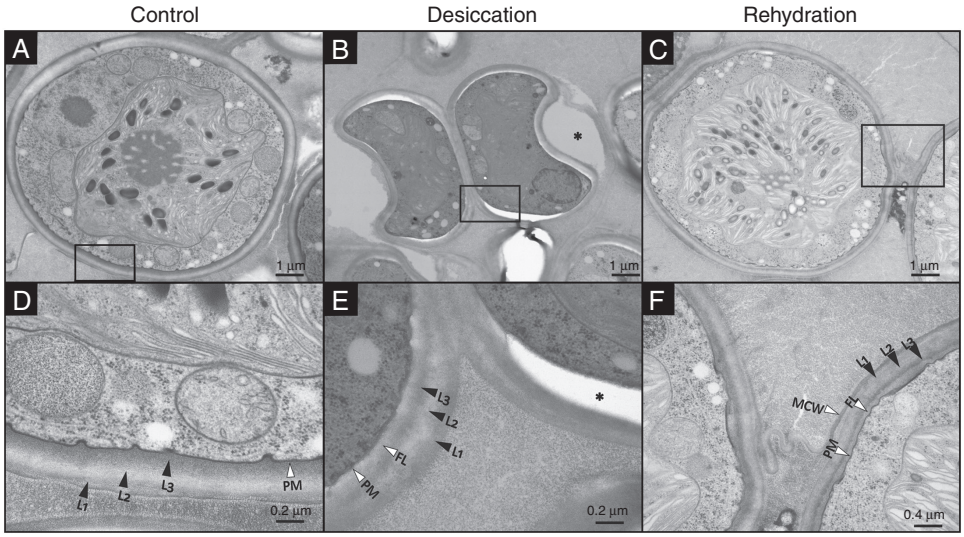

FIG. 4. TEM micrographs of TR9 sections with CW details during a D/R cycle. Rectangles in panels (A–C) indicate the areas shown at greater magnification in panels (D–F), respectively. The asterisk in (E) indicates a gap between the Epon 812 resin and the CW, probably due to reduced adherence of the collapsed regions to the resin. L1, L2 and L3 indicate the diffuse three-layer structure of the CW. FL, fibrillar layer; PM, plasma membrane; MCW, mother cell wall.

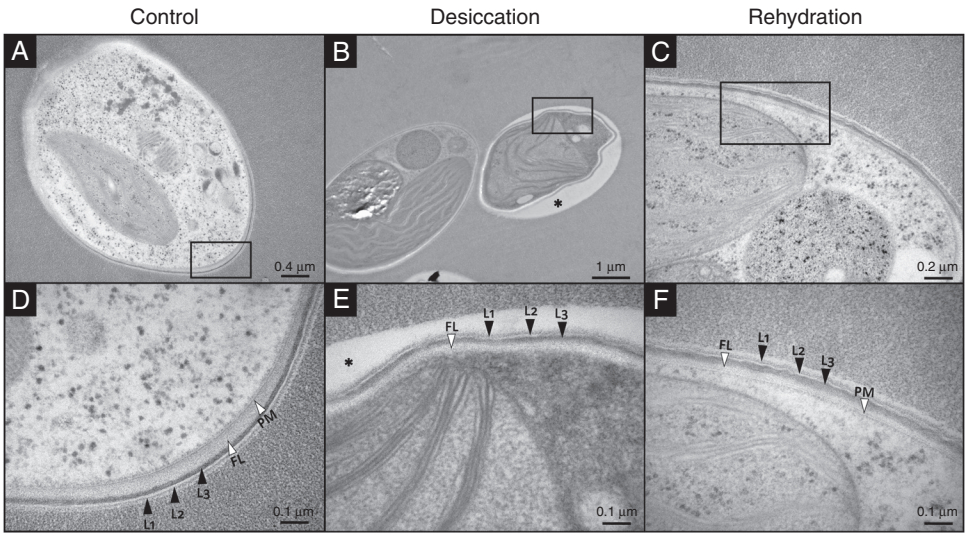

FIG. 5. TEM micrographs of Csol sections with CW details during a D/R cycle. Rectangles in panels (A–C) indicate the areas shown at higher magnification in panels (D–F), respectively. The asterisk in (B) and (E) indicates a gap between the Epon 812 resin and the CW, probably due to reduced adherence of the collapsed regions to the resin. L1, L2 and L3 indicate the typical three-laminar organization of the CW. FL, fibrillar layer; PM, plasma membrane.

significantly during D/R (Fig. 4 C, F and Supplementary Data Fig. S4). In contrast, the CW thickness of Csol decreased significantly during desiccation and recovered upon rehydration, but no apparent changes in its well-defined trilaminar structure were observed under D/R (Fig. 5 and Supplementary Data Fig. S4). In desiccation-tolerant moss protonemata, dehydration induces marked cytological alterations, including CW folding and changes in thickness (Pressel and Duckett, 2010).

Early studies on drying seeds by Webb and Arnott (1982) revealed that the 'controlled collapse' of the CW was necessary to maintain structural organization and cell viability in the desiccated state. Importantly, they found that CW deformation occurred in a species-specific manner and was related to the biochemical composition of the CW. This notion has now been extended to other desiccation-tolerant organisms (Shtein *et al.*, 2018), such as resurrection plants, in which the presence of plasticizing polysaccharides such as arabinans confers high flexibility on their CWs (Moore *et al.*, 2008*a*).

Cell wall biochemistry

Cell wall polysaccharides are constantly remodelled by several enzymes to adjust CW mechanical properties to changes in internal and external environmental conditions (Simmons *et al.*, 2015 and references therein). The ultrastructural adjustments observed in TR9 and Csol CWs during D/R strongly suggest that at least some of the main CW components were subjected to biochemical remodelling. Therefore, we conducted a comparative analysis of the polysaccharides in CW fractions from the two microalgae.

Fractionation of the CW yielded a significantly higher proportion of alkali-soluble (KOH) than hot-water-soluble (HW) polysaccharides in both TR9 and Csol under control conditions (T0). However, the KOH fraction in TR9 was 3.3 times higher than the HW one, whereas in Csol the latter was only 1.4 times higher than the former (Table 1). Exposure to four D/R cycles increased the proportion of HW polysaccharides in TR9, which contrasted with the reduction of both fractions in Csol.

The gel permeation profile of sugar-containing polymers in the HW fraction showed a main sharp peak of ~75 kDa in TR9 (Fig. 6A, peak 1) under control conditions (Table 1). After D/R cycles, we observed a marked shift in polymer distribution towards molecules of higher (to a greater extent) and lower molecular mass than 75 kDa (Fig. 6 A, Table 1). Previous glycosyl composition and linkage analyses of the crude CW of (control) TR9 algae indicated the predominance of a 3-linked galactofuranan substituted at the 6 position by rhamnosyl residues (Casano *et al.*, 2015). In this study, the polysaccharide(s) corresponding to peak 1 obtained by gel filtration chromatography of HW polymers showed galactose,

Table 1. *Effects of cyclic D/R on yield, molecular mass and glycosyl composition of cell wall polysaccharides of TR9 and Csol phycobionts. Cell walls were isolated before (T0) and after four D/R cycles, and fractionated sequentially with hot water (HW) and alkali (KOH). Each fraction was submitted to gel filtration chromatography on a Sepharose 4B column. Glycosyl composition analysis of selected fractions was performed by combined GC–MS of the per-*O*-trimethylsilyl derivatives of the monosaccharide methyl glycosides (Santander et al., 2013)*

Species	Treatment	Fraction	Fraction yield (% of CW mass)	Selected peak	Average molecular mass (kDa)	Monosaccharides (mol %)						
						Ara	Rha	Fuc	Xyl	Man	Gal	Glc
TR9	T0	HW	10.6	1	75	3.4	10.1	–	4.1	3.2	55.0	24.3
		KOH	35.6	3	174	1.3	23.6	–	39.5	0.6	30.7	4.4
	D/R	HW	14.6	2	103	–	32.5	–	8.0	–	59.5	–
		KOH	34.2	4	19	4.3	10.9	–	49.6	3.6	29.6	1.9
Csol	T0	HW	13.5	5	47	3.7	18.6	18.6	30.5	17.0	8.0	
		KOH	18.6	6a	174	–	–	–	–	–	4.5	95.5
				6b	61	–	4.5	4.7	8.3	–	6.4	76.1
				6c	5.2	1.2	1.5	7.3	7.8	9.1	8.1	65.2
	D/R	HW	5.5	–								
		KOH	10.1	7a	103	–	–	–	–	20.5	15.4	64.1
				7b	3.7	–	–	–	–	–	–	100

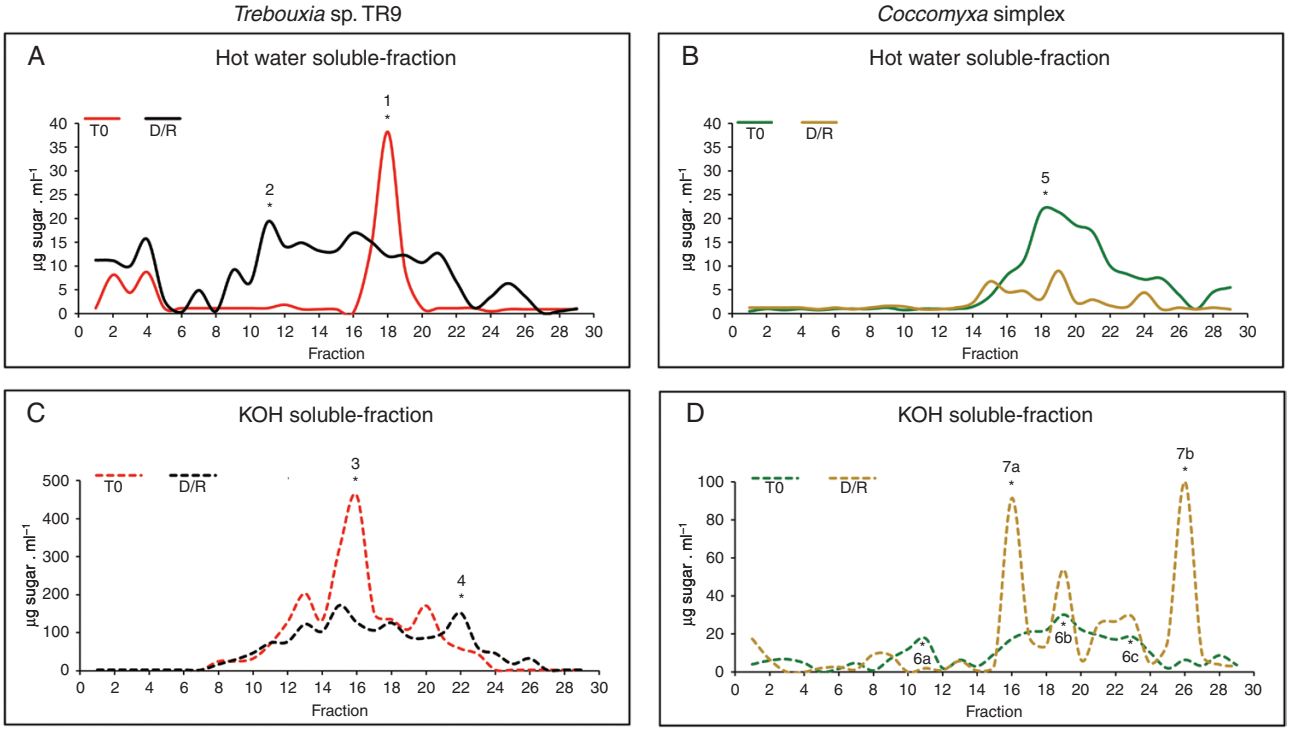

Fig. 6. Effects of four D/R cycles on the molecular mass profile of polysaccharides present in CW fractions of TR9 and Csol microalgae. Sepharose 4B chromatography of polysaccharides from each CW fraction was performed at least three times with at least two different CW preparations from independent TR9 and Csol cultures, under both control and D/R conditions. The chromatographic profile of each polysaccharide fraction did not differ by more than 5 % (in molecular mass) among replicates and with respect to those depicted in the figure. T0 corresponds to cell wall fractions before submitting to D/R cycles. The asterisks indicate fractions selected for glycosyl composition and glycosyl linkage analyses.

TABLE 2. *Glycosyl linkage analysis of CW polysaccharides of TR9 and Csol microalgae before and after cyclic D/R. Peak fractions of gel permeation chromatography were dialysed, freeze-concentrated, permethylated, depolymerized, reduced and acetylated. The resulting partially methylated alditol acetates were analysed by GC–MS as described by York et al. (1985). Peaks 2 and 5 corresponded to hot-water-soluble polysaccharides and peaks 4, 6 and 7 to KOH-soluble ones (for details see Table 1)*

Linkage	*Trebouxia sp. TR9*		*Coccomyxa simplex*					
	Peak 2	Peak 4	Peak 5	Peak 6a	Peak 6b	Peak 6c	Peak 7a	Peak 7b
	(mol %)							
t-Ara*f*	–	0.8	–	–	–	–	–	–
t-Xyl*p*	5.7	3.0	3.5	2.1	1.1	–	–	–
2-Rha*p*	10.9	1.2	7.9	3.1	0.7	–	–	–
t-Rha*p*	–	–	1.3	0.3	–	–	–	–
2-Man*p*	–	–	3.7	1.5	1.1	–	0.8	–
3-Rha*p*	–	1.3	13.8	6.6	2.0	–	–	–
t-Man*p*	–	–	0.4	0.1	1.3	–	–	–
3-Man*p*	–	–	bql	bql	bql	–	2.9	–
t-Glc*p*	6.1	0.5	–	4.3	7.1	16.9	48.1	91.2
t-Fuc*p*	–	–	4.0	–	0.1	–	–	–
3-Fuc*p*	–	–	–	0.3	1.9	–	3.8	–
t-Gal*f*	–	10.4	–	0.6	–	–	–	–
4-Fuc*p*	–	–	–	0.5	–	–	–	–
3,4-Fuc*p*	–	–	5.6	6.7	3.5	–	–	–
t-Gal*p*	–	1.2	2.0	1.1	4.9	–	–	–
3-Ara*p*	–	–	4.3	2.7	–	–	–	–
3-Ara*p* or 4-Ara*f*	–	–	–	–	1.6	–	–	–
t-Ara*p*	–	–	0.9	0.9	0.2	–	–	–
3-Xyl*p*	–	–	2.0	2.0	0.9	–	–	–
4-Xyl*p*	–	1.2	4.4	5.8	3.1	11.0	–	–
2-Rha*p*	–	–	7.9	–	–	–	–	–
3,4-Rha*p*	–	–	1.5	0.4	–	–	–	–
2,3-Rha*p*	14.7	1.1	6.0	4.2	0.5	–	–	–
2-Glc*p*	–	–	2.4	–	–	–	–	–
3-Glc*p*	–	–	–	0.3	0.4	–	–	–
3-Glc*f*	–	–	2.1	1.8	–	–	–	–
4-Rha*p*	–	–	–	–	–	–	–	–
4-Man*p*	–	5.9	–	0.9	2.5	8.7	8.4	–
3-Gal*f*	53.2	–	–	0.8	–	–	–	–
3-Hex*f**	–	21.5	–	–	–	–	–	–
4-Gal*p*	1.5	31.3	1.4	0.5	1.5	–	2.0	–
4-Glc*p*	5.3	1.4	3.2	26.0	42.0	57.4	27.1	8.8
6-Gal*f*	2.7	–	–	–	–	–	–	–
6-Glc*p*	–	–	–	–	0.5	–	–	–
6-Gal*p*	–	–	7.1	3.2	3.8	–	6.9	–
6-Man*p*	–	–	0.1	–	0.3	–	–	–
6-Hex*f**	–	2.8	–	–	–	–	–	–
3-Gal*p*	–	–	0.8	–	3.0	5.9	–	–
2,3-Glc*p*	–	2.1	–	–	–	–	–	–
2,4-Glc*p*	–	–	–	0.5	1.4	–	–	–
2,3-Man*p*	–	–	1.0	1.0	0.5	–	–	–
2,4-Man*p*	–	–	9.4	4.2	2.5	–	–	–
2,6-Man*p*	–	0.3	0.1	–	–	–	–	–
3,4-Man*p*	–	–	0.7	0.5	–	–	–	–
3,6-Man*p*	–	–	–	–	0.6	–	–	–
2,3,6-Man*p*	–	–	0.1	0.1	bql	–	–	–
2,4,6-Man*p*	–	–	0.4	0.3	0.5	–	–	–
3,4,6-Man*p*	–	–	7.5	1.0	4.8	–	–	–
3,4-Gal*p*	–	1.0	–	–	–	–	–	–
3,6-Gal*p*	–	1.4	1.6	0.2	0.6	–	–	–
3,6-Hex*f**	–	2.2	–	–	–	–	–	–
4,6-Gal*p*	–	9.0	0.3	–	–	–	–	–
3,4-Glc*p*	–	–	–	5.0	4.0	–	–	–
4,6-Glc*p*	–	–	0.3	5.1	4.0	–	–	–
2,3,4-Glc*p*	–	–	–	0.6	06	–	–	–
3,4,6-Gal*p*	–	0.5	–	–	–	–	–	–
3,4,6-Glc*p*	–	–	–	1.0	0.6	–	–	–

*Probably galactofuranosyl residues; – not detected; bql, below the quantification level.

glucose and rhamnose as the main monosaccharides (Table 1). Although the amount of carbohydrate recovered from peak 1 was insufficient to perform a glycosyl linkage analysis, its high galactose and rhamnose content resembled that of 3-linked galactofuranan. This is in line with the observation that the polydispersion caused by exposure to D/R cycles generated a peak of high molecular mass (peak 2, Fig. 6 A) predominantly formed by 2,3-linked galactofuranosyl and 2,3-linked rhamnopyranosyl residues (Table 2).

Under control conditions, the KOH fraction of TR9 showed polymers ranging from 146 to 47 kDa with a main peak at 103 kDa (Fig. 6 C, Table 1). Exposure to cyclic D/R did not seem to significantly alter the molecular mass pattern of the total polymers in TR9, except for the appearance of a low molecular mass peak (peak 4, Fig. 6 C, Table 1). A glycosyl composition analysis of peak 3 (control TR9) revealed a high content of xylose besides galactose and rhamnose (Table 1). Peak 4 showed an increased proportion of xylose and a lower content of rhamnose compared with KOH, under control conditions (Table 1). A methylation analysis showed that peak 4 consisted of a 4-linked galactopyranan substituted at *O*-6, *O*-3 and *O*-3,6 positions, a 3-linked galactofuranan and 4-linked xylopyranosyl molecules (Table 2).

A quite different scenario was found in HW and KOH polysaccharides from the Csol CW. Under control conditions, polysaccharide polydispersion was observed in both fractions, with a prevalence of medium to lower molecular mass polymers in the HW fraction, ranging from 103 to 4.3 kDa (Fig. 6 B), and a broader dispersion in the KOH fraction (Fig. 6 D). No marked qualitative changes in the molecular mass pattern of HW sugar-containing polymers was found as a consequence of cyclic D/R, but we did observe a generalized decrease in their abundance (Fig. 6 B), which is consistent with the reduced yield of the HW fraction (Table 1).

According to Centeno *et al.* (2016), glucose, mannose, galactose and rhamnose are the predominant neutral sugars present in the crude CW of Csol, although arabinose, xylose and fucose are also present. Glycosyl linkage analysis indicated the presence of a non-branched glucan with the main chain composed of 4-linked glucopyranosyl residues and a 4-linked mannan poorly substituted at the *O*-2 or *O*-3 position, probably by galactosyl or mannosyl residues. In the present study, HW peak 5 was mainly composed of xylose and almost equal proportions of rhamnose, fucose and mannose (Table 1). The glycosyl linkage analysis suggested the presence of linear xylans, as indicated by the presence of 3- and 4-Xyl*p* residues and two mannans: a 2-linked polymer highly substituted mainly at position 4 and a 3-linked one highly branched at the 4- and 6-positions in this peak (Table 2). Within the KOH-soluble polymers of control Csol, peak 6a presented a high proportion of glucose followed by a lower amount of galactose (Table 1), which seemed to compose a 4-linked glucan branched at *O*-3 and *O*-6 positions. The existence of 4-Gal*p* and 3-Gal*f* residues indicated the presence of galactans as minor components of this peak (Table 2). Peak 6b appeared to contain a 4-linked glucan similar to that found in peak 6a but less branched (one substitution at every ten Glc*p* residues, instead of every five residues) (Table 2). A linear 4-linked glucan was the main component of peak 6c, but 4-linked xylan and mannan and a 3-linked galactan were also found in lower amounts.

In contrast to what was observed in the HW fraction, exposure to cyclic D/R significantly altered the molecular size pattern of KOH polymers in the Csol CW, changing from a polydisperse distribution under control conditions to some sharp peaks from 103 to 3.7 kDa (peaks 7a and 7b, respectively, Fig. 6 D, Table 1) after D/R. Glucose was the main component of peak 7a, which seemed to be represented by a polymer of 4-linked Glc*p*. Polysaccharides formed by 4-Man*p* and 6-Gal*p* were also found in peak 7a (Table 2). Meanwhile, peak 7b was almost exclusively formed by a glucan, in which the high proportion of t-Glc*p* residues suggested the presence of amylose-like polysaccharide (Tables 1 and 2). Amylose has been reported as a polymer that adheres to CWs during polysaccharide extraction from lichen phycobionts (Cordeiro *et al.*, 2008).

Results from the present study confirm our previous findings with crude CWs of the same microalgae under control conditions (Casano *et al.*, 2015; Centeno *et al.*, 2016) and extend them towards a more detailed analysis of CW components and how these are modified in response to cyclic D/R. Farrant *et al.* (2017) recently reported that the flexibility of *Craterostigma wilmsii* CWs seems to be modulated during desiccation. The proportion of glucose decreases and that of galactose increases as substituent in xyloglycans. These polysaccharides also change their degree of polymerization, moving from large to shorter chains and thus increasing CW flexibility under desiccation conditions (Farrant *et al.*, 2017). In our study, an analogous remodelling was observed due to changes in the alkaline-soluble polysaccharides extracted during the relatively slow and mild desiccation of Csol. In contrast, more marked changes were observed in the TR9 water-soluble fraction during fast and drastic desiccation, as the main medium molecular mass polysaccharide found in control cells changed to a complex mixture of different-sized polysaccharides. After D/R cycles, the degree of polymerization of Csol β-glucans decreased. Biochemical remodelling of the CW appears to play a crucial role in controlling its biomechanical properties, helping lichen microalgae to cope with rapid changes in the cell's hydric status. This study also supports the notion that CW remodelling is an active and species-specific process, induced by exposure to desiccation conditions similar to those encountered in the natural habitats in which each alga/lichen thrives.

SUPPLEMENTARY DATA

Supplementary data are available online at https://academic.oup.com/aob and consist of the following. Figure S1: extended TEM micrograph of TR9 under control conditions, showing detail of characteristic invaginations. Fig. S2: extended LTSEM micrograph of TR9 under desiccation conditions. Fig. S3: microscopic images of TR9 and Csol cells stained with 0.2 % crystal violet for 24 h. Fig. S4: effects of desiccation and rehydration on cell wall thickness of Csol and TR9 microalgae.

FUNDING

This research was supported by grants from the Spanish Ministry of Science, Innovation and Universities (CGL2016-80259-P), (PGC2018-094076-B-I00 to C.A.), Fundação de Amparo a Pesquisa do Estado de São Paulo, Brazil (2017/50341-0 to M.R.B.) and Conselho Nacional de Desenvolvimento Científico e Tecnológico, Brazil (305542/2016–8 to M.R.B.).

ACKNOWLEDGEMENTS

We thank Parastoo Azadi at the Complex Carbohydrate Research Center for glycosyl composition and linkage analyses, which were partially supported by a grant from the Chemical Sciences, Geosciences and Biosciences Division, Office of Basic Energy Sciences, U.S. Department of Energy (DE-SC0015662). ESEM and LTSEM observations were conducted under the guidance of Dr Sanchez Almazo at the Microscopy Service, Granada University Centre for Scientific Instrumentation (Spain).

LITERATURE CITED

Aichinger N, Lütz-Meindl U. 2005. Organelle interactions and possible degradation pathways visualized in high-pressure frozen algal cells. *Journal of Microscopy* **219**: 86–94.

Álvarez R, del Hoyo A, Díaz-Rodríguez C, *et al.* 2015. Lichen rehydration in heavy metal polluted environments: Pb modulates the oxidative response of both *Ramalina farinacea* thalli and its isolated microalgae. *Microbial Ecology* **69**: 698–709.

Aragón G, Belichón M, Martínez I, Prieto M. 2016. A survey method for assessing the richness of epiphytic lichens using growth forms. *Ecological Indicators* **62**: 101–105.

Ascaso C, Sancho LG, Rodríguez-Pascual C. 1990. The weathering action of saxicolous lichens in maritime Antarctica. *Polar Biology* **11**: 33–39.

Aschenbrenner IA, Cardinale M, Berg G, Grube M. 2014. Microbial cargo: do bacteria on symbiotic propagules reinforce the microbiome of lichens? *Environmental Microbiology* **16**: 3743–3752.

Belnap J, Büdel B, Lange OL. 2001. Biological soil crusts: characteristics and distribution. In: Belnap J, Lange OL, eds. *Biological soil crusts: structure, function, and management*. Berlin: Springer, 3–30.

Bold HC, Parker BC. 1962. Some supplementary attributes in the classification of *Chlorococcum* species. *Archiv Für Mikrobiologie* **42**: 267–288.

Casano LM, del Campo EM, García-Breijo FJ, *et al.* 2011. Two *Trebouxia* algae with different physiological performances are ever-present in lichen thalli of *Ramalina farinacea.* Coexistence versus competition? *Environmental Microbiology* **13**: 806–818.

Casano LM, Braga MR, Álvarez R, del Campo EM, Barreno E. 2015. Differences in the cell walls and extracellular polymers of the two *Trebouxia* microalgae coexisting in the lichen *Ramalina farinacea* are consistent with their distinct capacity to immobilize extracellular Pb. *Plant Science* **236**: 195–204.

Centeno DC, Hell AF, Braga MR, del Campo EM, Casano LM. 2016. Contrasting strategies used by lichen microalgae to cope with desiccation-rehydration stress revealed by metabolite profiling and cell wall analysis. *Environmental Microbiology* **18**: 1546–1560.

Cordeiro LMC, Carbonero ER, Sassaki GL, *et al.* 2005. A fungus-type β-galactofuranan in the cultivated *Trebouxia* photobiont of the lichen *Ramalina gracilis*. *FEMS Microbiology Letters* **244**: 193–198.

Cordeiro LMC, de Oliveira SM, Buchi DF, Iacomini M. 2008. Galactofuranose-rich heteropolysaccharide from Trebouxia sp., photobiont of the lichen Ramalina gracilis and its effect on macrophage activation. *International Journal of Biological Macromolecules* **42**: 436–440.

Cordeiro LMC, Sassaki GL, Iacomini M. 2007. First report on polysaccharides of *Asterochloris* and their potential role in the lichen symbiosis. *International Journal of Biological Macromolecules* **41**: 193–197.

Dubois M, Gilles KA, Hamilton JK, Rebers PA, Smith F. 1956. Colorimetric method for determination of sugars and related substances. *Analytical Chemistry* **28**: 350–356.

Dunker S, Wilhelm C. 2018. Cell wall structure of coccoid green algae as an important trade-off between biotic interference mechanisms and multidimensional cell growth. *Frontiers in Microbiology* **13**: 719.

Farrant JM, Cooper K, Dace HJW, Bentley J, Hilgart A. 2017. Desiccation tolerance. In: Shabala S, ed. *Plant stress physiology*. Boston: CABI Publishers, 217–252.

Fritsch F, Haines F. 1923. The moisture-relations of terrestrial algae. II. The changes during exposure to drought and treatment with hypertonic solutions. *Annals of Botany* **37**: 683–728.

Gaff DF. 1971. Desiccation-tolerant flowering plants in southern Africa. *Science* **174**: 1033–1034.

Gasulla F, Guéra A, Barreno E. 2010. A simple and rapid method for isolating lichen photobionts. *Symbiosis* **51**: 175–179.

Heiss C, Stacey Klutts J, Wang Z, Doering TL, Azadi P. 2009. The structure of *Cryptococcus neoformans* galactoxylomannan contains β-D-glucuronic acid. *Carbohydrate Research* **344**: 915–920.

Hell AF, Gasulla F, González-Hourcade M, del Campo EM, Centeno DC, Casano LM. 2019. Tolerance to cyclic desiccation in lichen microalgae is related to habitat preference and involves specific priming of the antioxidant system. *Plant & Cell Physiology* **60**: 1880–1891.

Holzinger A, Karsten U. 2013. Desiccation stress and tolerance in green algae: consequences for ultrastructure, physiological and molecular mechanisms. *Frontiers in Plant Science* **4**: 327.

Holzinger A, Pichrtová M. 2016. Abiotic stress tolerance of charophyte green algae: new challenges for omics techniques. *Frontiers in Plant Science* **7**: 678.

Honegger R. 2012. The symbiotic phenotype of lichen-forming Ascomycetes and their endo- and epibionts. In: Hock B, ed. *Fungal associations*, 2nd edn. Berlin: Springer, 287–339.

Honegger R, Brunner U. 1981. Sporopollenin in the cell walls of *Coccomyxa* and *Myrmecia* phycobionts of various lichens: an ultrastructural and chemical investigation. *Canadian Journal of Botany* **59**: 2713–2734.

König J, Peveling E. 1984. Cell walls of the phycobionts *Trebouxia* and *Pseudotrebouxia*: constituents and their localization. *The Lichenologist* **16**: 129–144.

Kranner I, Beckett R, Hochman A, Nash TH. 2008. Desiccation-tolerance in lichens: a review. *The Bryologist* **111**: 576–593.

Molins A, García-Breijo FJ, Reig-Armiñana J, del Campo EM, Casano LM, Barreno E. 2013. Coexistence of different intrathalline symbiotic algae and bacterial biofilms in the foliose Canarian lichen *Parmotrema pseudotinctorum*. *Vieraea* **41**: 349–370.

Moore JP, Nguema-Ona E, Chevalier L, *et al.* 2006. Response of the leaf cell wall to desiccation in the resurrection plant *Myrothamnus flabellifolius*. *Plant Physiology* **141**: 651–662.

Moore JP, Farrant JM, Driouich A. 2008*a*. A role for pectin-associated arabinans in maintaining the flexibility of the plant cell wall during water deficit stress. *Plant Signaling and Behavior* **3**: 102–104.

Moore JP, Vicré-Gibouin M, Farrant JM, Driouich A. 2008*b*. Adaptations of higher plant cell walls to water loss: drought vs desiccation. *Physiologia Plantarum* **134**: 237–245.

Pressel S, Duckett JG. 2010. Cytological insights into the desiccation biology of a model system: moss protonemata. *New Phytologist* **185**: 944–963.

Santander J, Martin T, Loh A, Pohlenz C, Gatlin D, Curtiss R. 2013. Mechanisms of intrinsic resistance to antimicrobial peptides of *Edwardsiella ictaluri* and its influence on fish gut inflammation and virulence. *Microbiology* **159**: 1471–1486.

Schroeter B, Green TGA, Seppelt RD, Kappen L. 1992. Monitoring photosynthetic activity of crustose lichens using a PAM-2000 fluorescence system. *Oecologia* **92**: 457–462.

Sherwin HW, Farrant JM. 1996. Differences in rehydration of three different desiccation tolerant species. *Annals of Botany*. **78**: 703–710.

Shtein I, Bar-On B, Popper ZA. 2018. Plant and algal structure: from cell walls to biomechanical function. *Physiologia Plantarum* **164**: 56–66.

Simmons TJ, Mohler KE, Holland C, Goubet F, Franková L, Houston DR, Hudson AD, Meulewaeter F, Fry SC. 2015. Hetero-trans-β-glucanase, an enzyme unique to Equisetum plants, functionalizes cellulose. *Plant Journal* **83**: 753–769.

Tuba Z, Csitanlan Z, Proctor M. 1996. Photosynthetic responses of a moss, *Tortula ruralis*, ssp. *Ruralis,* and the lichens *Cladonia convolute* and *C. Furcata* to water deficit and short periods of desiccation, and their ecophysiological significance: a baseline study at present-day CO2 concentration. *New Phytologist* **133**: 353–361.

Vargas Castillo R, Stanton D, Nelson PR. 2017. Aportes al conocimiento de la biota liquénica del oasis de neblina de Alto Patache, desierto de Atacama. *Revista de Geografía Norte Grande* **68**: 49–64.

Vicré M, Lerouxel O, Farrant J, Lerouge P, Driouich A. 2004. Composition and desiccation-induced alterations of the cell wall in the resurrection plant *Craterostigma wilmsii*. *Physiologia Plantarum* **120**: 229–239.

Webb M, Arnott H. 1982. Cell wall conformation in dry seeds in relation to the preservation of structural integrity during desiccation. *American Journal of Botany* **69**: 1657–1668.

York WS, Darvill AG, McNeil M, Stevenson TT, Albersheim P. 1985. Isolation and characterisation of plant cell walls and cell wall

components. In: Weissbach A, Weissbach H, eds. *Methods in enzymology*, Orlando: Academic Press Inc., 3–40.

Zhang T, Wei XL, Zhang YQ, Liu HY, Yu LY. 2015. Diversity and distribution of lichen-associated fungi in the Ny-Ålesund Region (Svalbard, High Arctic) as revealed by 454 pyrosequencing. *Scientific Reports* **5**: 14850.

Zhang Z, Volkman JK. 2017. Algaenan structure in the microalga *Nannochloropsis oculata* characterized from stepwise pyrolysis. *Organic Geochemistry* **104**: 1–7.

Zych M, Burczyk J, Kotowska M, *et al.* 2009. Differences in staining of the unicellular algae Chlorococcales as a function of algaenan content. *Acta Agronomica Hungarica*. **57**: 377–381.